

CME Article

Clinics in diagnostic imaging (I23)

Wong S B S, Peh W C G, Lim S L



Fig. 1 Lateral radiograph of the thoracic spine.

Fig. 2 Sagittal (a) SET1-WW, (b) STIR and (c) contrast-enhanced fat-suppressed SET1-WW MR images of the thoracic spine.

CASE PRESENTATION

A 60-year-old Indian man presented to the Accident and Emergency Department with bilateral lower limb weakness, after sustaining a fall in a toilet three days prior. He gave a history of landing on his buttocks, and experienced back pain and progressive lower limb weakness. He denied having any numbness or incontinence. On physical examination, he had no saddle anaesthesia and his anal tone was normal. Although power was reduced in both lower limbs, he could tolerate straight leg raising to up to 50 degrees bilaterally, and had

normal brisk reflexes and sensation. On palpation, he was noted to be tender over the lower thoracic spine and both paraspinal regions. He was afebrile on admission.

Radiographs of his spine were performed (Fig. 1). His blood tests on admission showed a total white cell count (TWC) of $9.1 \times 10^9/L$, haemoglobin (Hb) of 12.7 g/dL, and normal international normalised ratio, prothrombin time and activated partial thromboplastin time. He was admitted and magnetic resonance (MR) imaging of the spine was performed (Figs. 2a–c). What are the imaging findings? What is the diagnosis?

Department
of Diagnostic
Radiology,
Alexandra Hospital,
378 Alexandra Road,
Singapore 159964

Wong SBS, MBChB,
MMed
Registrar

Peh WCG, MD,
FRCP, FRCR
Clinical Professor and
Senior Consultant

Department of
Orthopaedic
Surgery

Lim SL, MBBS,
FRCS
Senior Consultant

Correspondence to:
Prof Wilfred CG Peh
Tel: (65) 9820 3717
Fax: (65) 6463 9649
Email: wilfred@
pehfamily.per.sg

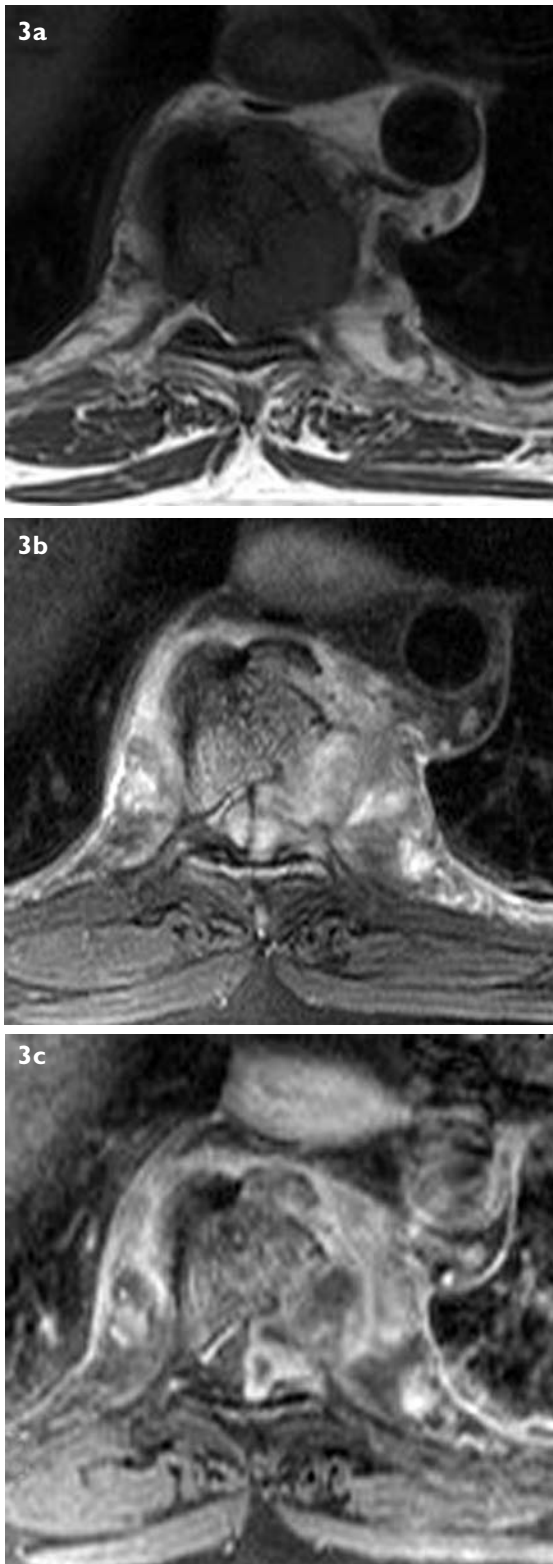


Fig. 3 Axial (a) SE T1-W, (b) fat-suppressed FSE T2-W and (c) contrast-enhanced fat-suppressed SET1-W MR images of the T8 vertebra show bilateral paraspinal abscesses, larger on the left side, with intraspinal extension. The spinal cord is indented and displaced to the right.

IMAGE INTERPRETATION

The lateral spine radiograph (Fig. 1) showed compression of T8 and T9 vertebral bodies with indistinct outlines of

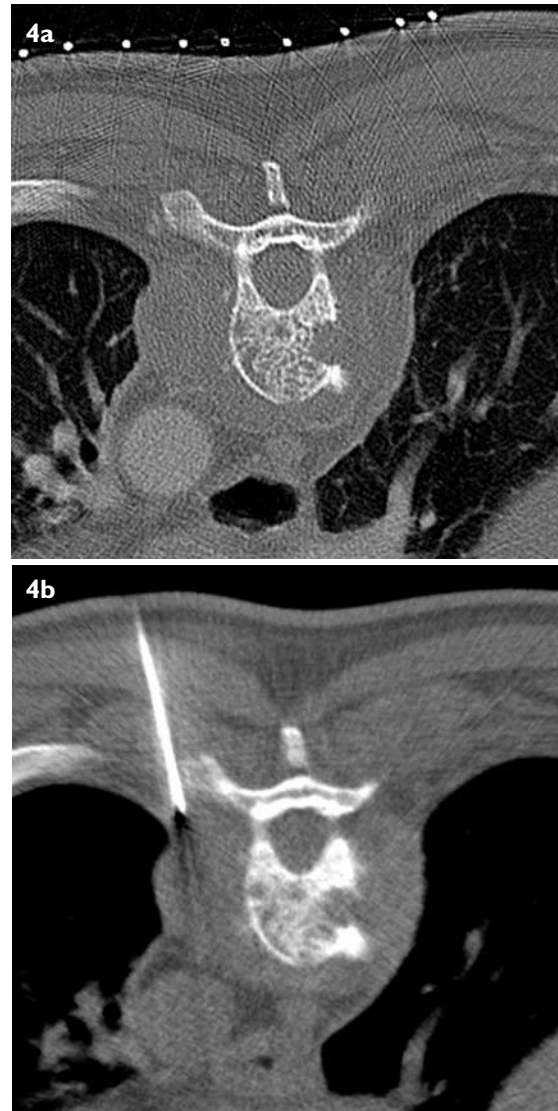


Fig. 4 Axial CT images, obtained with the patient lying prone, taken (a) before and (b) during CT-guided biopsy show the targeted prominent left paraspinal soft tissue mass and the biopsy needle's location. Note the mottled osteolytic appearance of the vertebral body, with a focal right lateral cortical destruction. The biopsy was performed at the T7/8 level.

the T7 lower endplate and T10 upper endplate. A mild kyphosis was evident. MR imaging of the thoracic spine (Fig. 2) showed moderately severe T8 and T9 vertebra compression fractures and of the adjoining T7 and T10 vertebral bodies. Rim-enhancing bilateral paraspinal collections, compatible with abscesses, were seen, with craniocaudal and intraspinal extensions. Anterior subligamentous soft tissue swelling was indicative of contiguous spread of the infection. Axial MR images (Figs. 3a–c) showed extension of the left paraspinal abscess into the spinal canal, from T7 to T11 levels, causing indentation of the spinal cord and displacing it to the right. The upper thoracic and the lumbar vertebrae showed no suspicious focal or global enhancement.

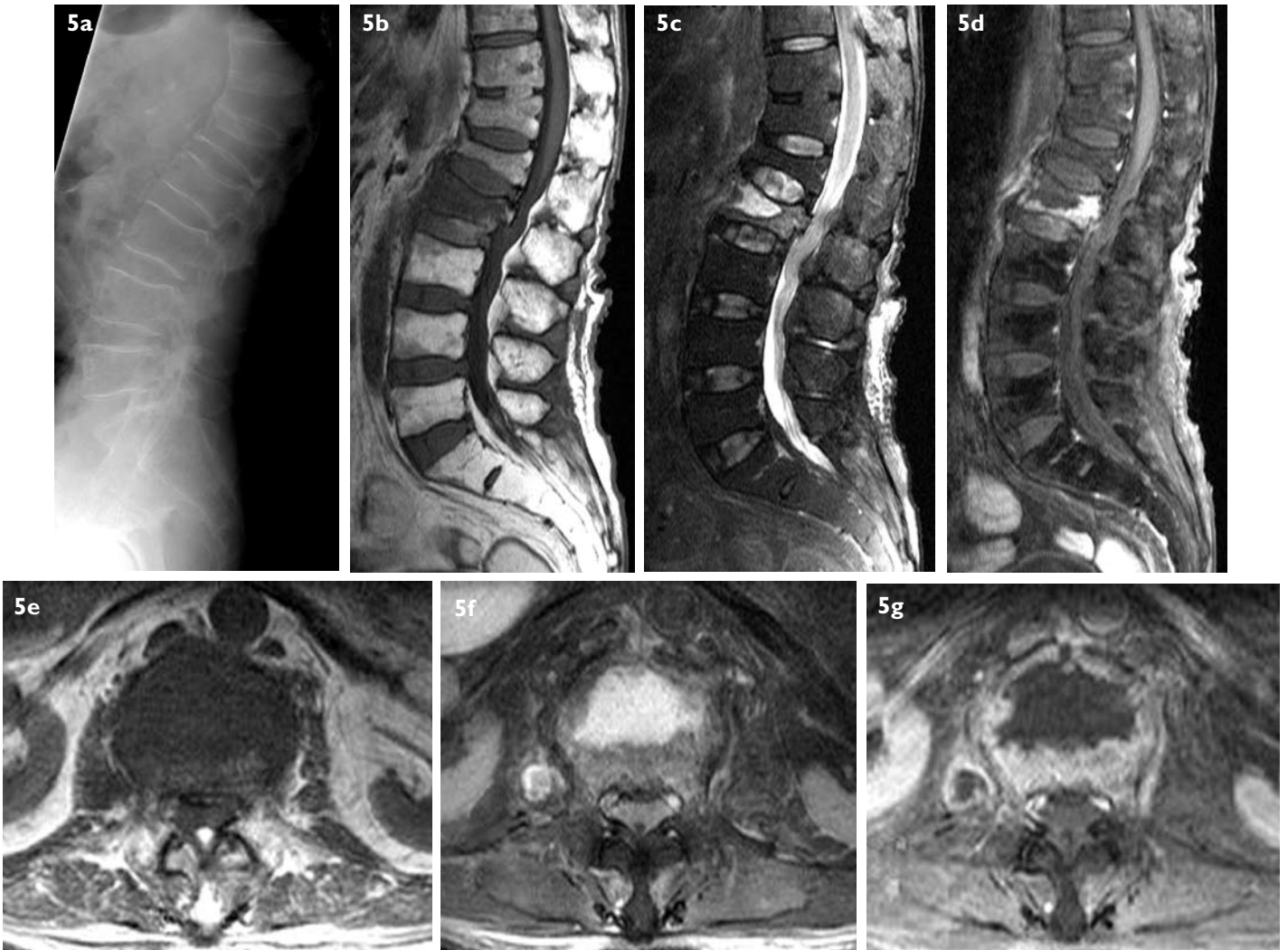


Fig. 5 L2 vertebral osteomyelitis and paraspinal abscesses in an ill 71-year-old man with methicillin-sensitive *Staphylococcus aureus* bacteraemia and who presented with acute middle to lower back pain. He had known previous T12 and L1 vertebral compression fractures. (a) Lateral spinal radiograph shows loss of definition of the anterior border of L2 vertebral body. Sagittal (b) SET1-W; (c) fat-suppressed FSE T2-W; (d) contrast-enhanced fat-suppressed SET1-W; and axial (e) SET1-W; (f) fat-suppressed FSE T2-W; (g) contrast-enhanced fat-suppressed SET1-W MR images show avid enhancement of the L2 vertebra, save for the anterior wedge-shaped area of T1-hypointensity and T2-hyperintensity, which is non-enhancing, consistent with an abscess. The anterior subligamentous enhancement is indicative of early abscess formation, accounting for the erosion of the anterior border.

DIAGNOSIS

Tuberculous spondylitis.

CLINICAL COURSE

The diagnosis was confirmed on histology with specimens obtained from a computed tomography (CT)-guided biopsy of the left paraspinal abscess (Fig. 4). Histological examination showed granulomatous inflammation with caseous necrosis, and positive Ziehl-Nielsen staining for acid-fast bacilli. Emergency spinal decompression was offered, but was declined by the patient. He was subsequently referred to the Infectious Disease Service and started on a nine-month course of anti-tuberculous therapy. During his three-week hospital stay, there was

a gradual increase in his TWC from $9.1 \times 10^9/L$ to $12.7 \times 10^9/L$, with a differential shift to marked neutrophilia. Erythrocyte sedimentation rate (ESR) was normal at 16 mm/hr and C-reactive protein (CRP) was mildly prominent at 7.6 mg/L. Molecular tuberculosis (TB) test was positive for *Mycobacterium tuberculosis*, confirming the histological findings. A myeloma screen was normal, and no abnormal bands were demonstrated on serum and urine electrophoresis. His glycosylated Hb was 7.1%. He was subsequently discharged to a nursing home for his convalescence.

DISCUSSION

This patient had the typical imaging findings of tuberculous spondylitis. Infective spondylitis classically



Fig. 6 Paraspinal soft tissue involvement in the same patient as in Figs. 1–4. Reformatted (a) coronal and (b) sagittal CT images show bilateral paraspinal soft tissue swelling. The T8 and T9 vertebral bodies have areas of increased sclerosis in areas and loss of height from infective destruction. The sagittal view shows the anterior subligamentous abscess well.

involves two adjacent vertebrae and the intervening intervertebral disc. Atypical presentations include that of a single vertebral involvement without discal abnormality (thought to represent an early stage of the infection), contiguous levels of vertebrae, and isolated infective focus in the posterior elements. Extension into the paraspinal soft tissues and epidural space may also occur.^(1,3)

Infective spondylitis constitutes 2%–4% of all cases of osteomyelitis.^(1,4) Males are more frequently affected than females, with a ratio of 2–3:1.^(1,4) The average age of presentation is in the fifth to sixth decade of life. Though less common and harder to diagnose in children, a bimodal age distribution is seen, peaking at six months to four years, and again at 10–14 years.⁽¹⁾ The lumbar spine is the most commonly-affected region, followed by the thoracic and cervical spine and rarely, the sacrum.⁽¹⁾ The thoracolumbar junction is a common site involved in tuberculous spondylitis.⁽⁴⁾ Multilevel involvement is commonly seen in the cervical spine, though the actual incidence remains higher in the thoracic and lumbar spine, by virtue of their higher incidence.⁽¹⁾

Potential routes of infection include haematogenous spread, both arterial and venous, direct contamination and direct spread from adjoining abscess. Arterial haematogenous spread from other sources of infection is particularly important, as it necessitates the exclusion or identification of a urinary tract infection, respiratory

infection or endocarditis.⁽²⁾ The arteries at the anterior aspect of the vertebra possess the richest supply, accounting for the initial infective focus in the anterior subchondral bone.⁽³⁾ The Batson's paravertebral venous plexus of valveless veins provides a potential route of retrograde spread from abdominal veins.^(1,3,4) Direct contamination of the discs or spine or spinal canal puncture may occur postsurgery, though the incidence is extremely low.

Causative organisms are myriad. In pyogenic spondylitis, the pre-dominant organism is *Staphylococcus aureus* (50%), particularly affecting male patients older than 50 years of age. Other gram-positive bacteria include *Streptococcus* and *Pneumococcus*. Gram-negative bacteria as a cause are less common and include *Eschericia coli*, *Pseudomonas*, *Klebsiella*, *Enterococcus* and *Salmonella*. *Pseudomonas aeruginosa* is common in intravenous drug users, though *S. aureus* is still the dominant organism in this group. *Salmonella* is an important consideration in children, and *Streptococcus* for patients with endocarditis.^(1,2,4,5) Among granulomatous infections, *Mycobacterium tuberculosis* is the most common cause, and shows an increasing incidence worldwide, followed by brucella.^(1,4) Less common organisms include fungal organisms like blastomycosis, coccidioidomycosis, aspergillosis, candidiasis, and parasites like echinococcus and toxoplasmosis.^(1,4,6,7)

Non-imaging diagnostic tests are generally non-



Fig. 7 Single-level discitis with osteomyelitis in a 47-year-old man with chronic low back pain, that was managed conservatively with antibiotics. Sagittal (a) SET1-W; (b) contrast-enhanced fat-suppressed T1-W; axial (c) fat-suppressed FSET2-W; (d) contrast-enhanced fat-suppressed T1-W; and (e) coronal contrast-enhanced fat-suppressed T1-W MR images show L2/3 discitis with L2 and L3 vertebral osteomyelitis. Paraspinal enhancement is clearly demonstrated. The L2/3 intervertebral disc protrudes into the spinal canal, with mild canal stenosis.

specific and include TWC, ESR and CRP levels. TWC is often inaccurate and can even remain normal in chronic infective spondylitis. CRP is now thought to be more sensitive than ESR, although both markers may be raised during infection. CRP has been shown to normalise more rapidly postsurgery or following appropriate treatment,

while ESR levels can remain persistently raised or even rise despite clinical improvement.⁽¹⁻³⁾ Specimens for microbiological studies should include blood and urine, at the minimum.

Radiographs are often normal in the early stage of infection (the first 1–3 weeks). Nonetheless, they are

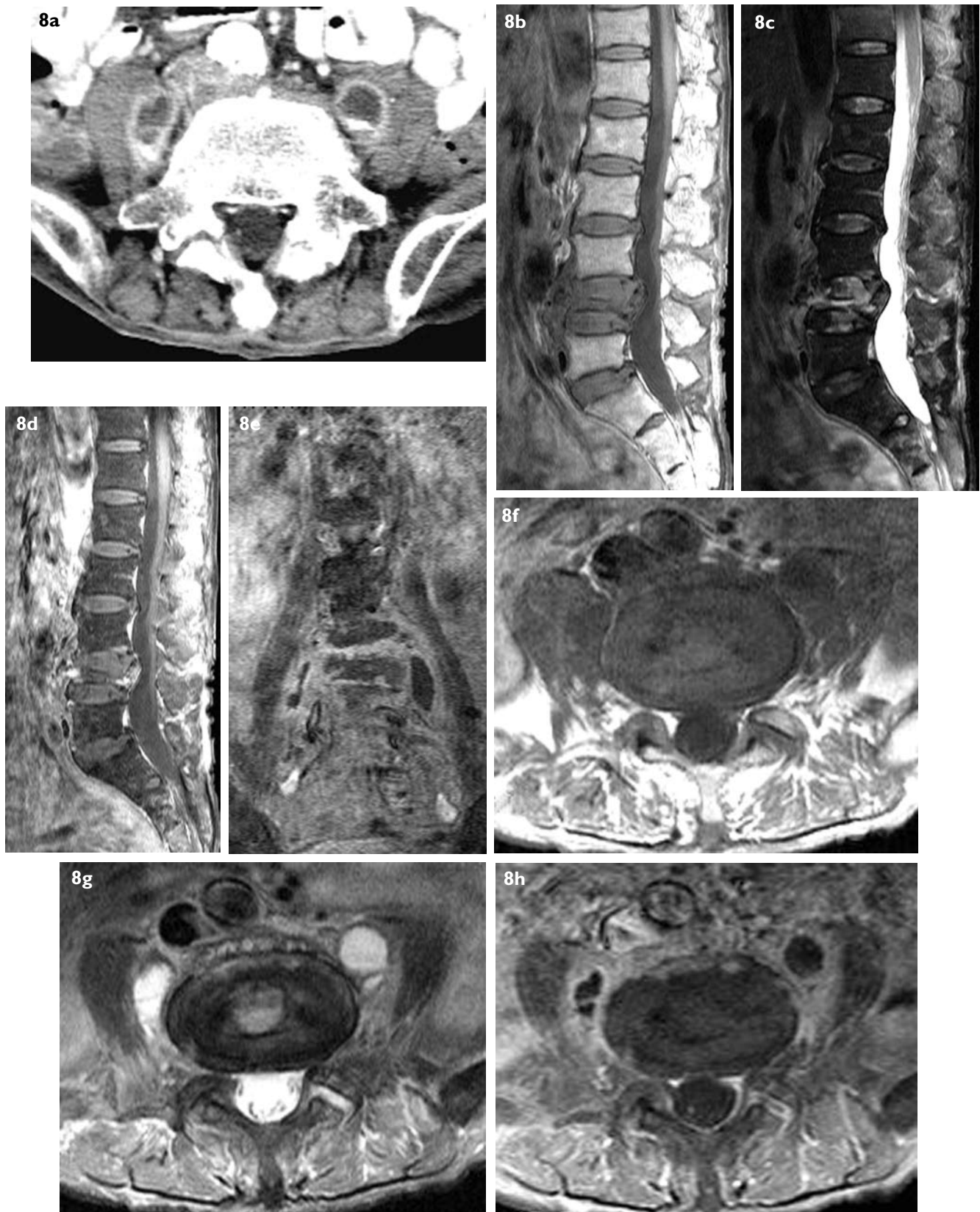


Fig. 8 Discitis and paraspinal abscesses in a 70-year-old man with known *Staphylococcus aureus* bacteraemia. (a) Axial contrast-enhanced CT image shows bilateral rim-enhancing psoas abscesses. Sagittal (b) SE T1-W; (c) fat-suppressed FSET2-W; (d) contrast-enhanced fat-suppressed T1-W; (e) coronal contrast-enhanced fat-suppressed T1-W; and axial (f) SE T1-W; (g) fat-suppressed FSET2-W; (h) contrast-enhanced fat-suppressed T1-W MR images show L4 vertebra plana with enhancement and swollen L3/4 and L4/5 intervertebral discs, secondary to infection. Retropulsed posterior fragment of the L4 vertebral body results in spinal canal stenosis at this level. Bilateral psoas rim-enhancing abscesses are best seen on axial and coronal images.

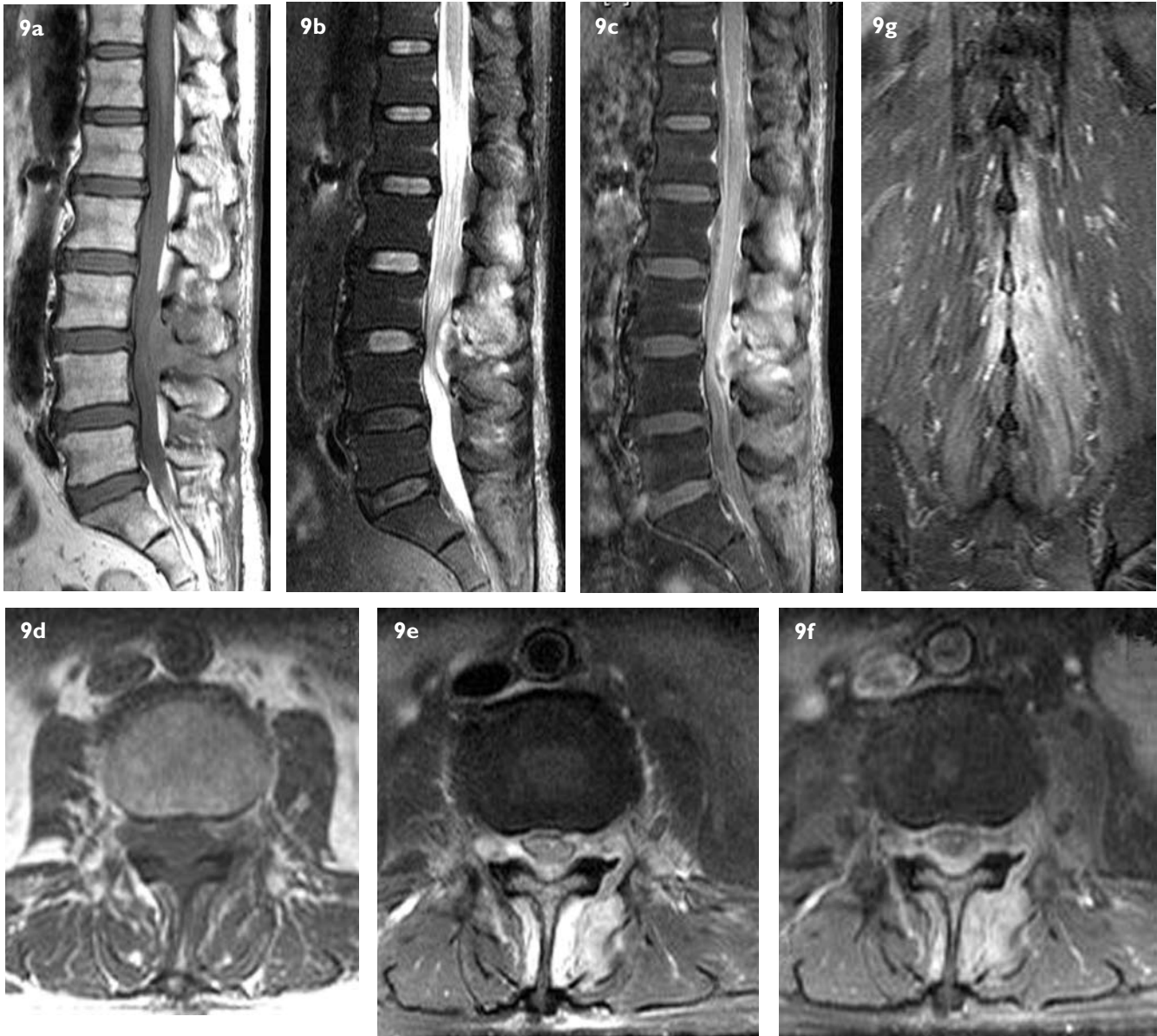


Fig. 9 Myositis and epidural abscesses in a 59-year-old woman with *Staphylococcus aureus* bacteraemia, and who had complaint of back pain during admission. Sagittal (a) SE T1-W; (b) fat-suppressed FSE T2-W; (c) contrast-enhanced fat-suppressed T1-W; axial (d) SE T1-W; (e) fat-suppressed FSE T2-W; (f) contrast-enhanced fat-suppressed T1-W; and (g) coronal contrast-enhanced fat-suppressed T1-W MR images show a small posterior intraspinal epidural abscess from mid-L3 to mid-L4 levels, causing posterior thecal sac compression. Enhancement of bilateral erector spinae muscles are suggestive of concurrent myositis. Surgical drainage of the posterior epidural abscess was performed, with resection of the L3 to L5 spinous processes.

useful in the initial assessment of possible disease at presentation, monitoring progression of disease, and to quickly evaluate existence of corresponding coronal or sagittal deformity. The initial signs include decreased disc height (seen in 75% of patients), usually within 2–3 weeks of infection, blurring of the endplates, particularly the anterior region, and medullary bone destruction in the adjacent vertebra.^(1,3,4) In some cases, discrete subchondral radiolucency is evident, particularly anteriorly,⁽⁴⁾ correlating with the arterial supply (Fig. 5a). Increase in disc height may be illusory and secondary to endplate destruction,⁽⁸⁾ though it has been seen in the

early spread of infection to the disc space with abscess formation.⁽¹⁾ Late changes include endplate sclerosis from reparative processes, bony ankylosis,⁽¹⁾ progressive kyphosis or scoliosis in chronic infection.⁽³⁾ Paraspinal soft tissue disease extension is often less evident or absent, with loss of the paravertebral stripe, loss of—or conversely, an enlarged—psoas shadow being clues to be detected.

CT effectively shows the changes mentioned above and in addition, is able to show the paravertebral fat effacement and intervertebral disc hypodensity in early infective spondylitis.⁽⁴⁾ CT will also more readily

demonstrate local extension in the paravertebral space, including paraspinal mass and epidural soft tissue mass, particularly with intravenous contrast enhancement.⁽¹⁾ Late features of infection, such as permeative bone destruction in the adjacent vertebral bodies, endplate erosions, sequestra and pathological calcification formation, can be diagnosed earlier with CT than on radiographs.⁽⁴⁾ Early endplate destruction may be missed on axial CT images, owing to partial volume averaging, though this problem has been overcome to a certain extent with the widespread usage of multi-detector CT scanners; this allows for coronal and sagittal multiplanar reconstructions⁽²⁾ (Fig. 6a & b). CT is inferior to MR imaging in the assessment of the spinal canal disease. One of the major roles of CT in current practice is to guide aspiration of paraspinal masses, bone biopsies (Fig. 4) and drainage of fluid collections.⁽¹⁾

MR imaging is currently the imaging modality of choice, given its superior ability in the detection of soft tissue and bone marrow changes, with a sensitivity of 96% and accuracy of 94% (Fig. 5). MR imaging of the entire spine should be performed to exclude multi-level involvement and skip vertebrae. Performing contrast-enhanced T1-weighted sequences with fat suppression provide valuable additional information and is highly recommended. Bone marrow oedema is a recognised early sign of infection. These are seen as areas of hypointensity on T1-weighted images, and hyperintense areas on T2-weighted, short tau inversion recovery (STIR) and proton density fat-suppressed sequences^(1,2,4) (Fig. 5). Early in the disease course, marrow signal changes may not be evident, though enhancement can be seen with post-contrast fat suppressed T1-weighted sequences.⁽¹⁾

Other MR imaging changes evident in the acute phase include T1-hypointensity with loss of definition of the endplates and adjacent vertebral bodies, and T2-hyperintense intervertebral discs and adjacent vertebral bodies. Vertebral endplate erosion is seen as loss of the normal T1-hypointense line on the sagittal MR images⁽¹⁾ (Fig. 7). Paradoxically, increased conspicuity of the endplates from pseudosparring has been described, due to marrow fat replacement and loss of the chemical shift artifact.⁽³⁾ The intervertebral disc space may show homogeneous T2-hyperintensity with loss of the normal intranuclear cleft, though this sign may be inconsistent.⁽⁵⁾ Discal enhancement patterns include homogeneous disc enhancement, patchy non-confluent areas of disc enhancement and varying areas of peripheral disc enhancement⁽³⁾ (Fig. 7). Reduced disc height and finding of T1-hypointensity, rather than the

usual isointensity, are additional findings.⁽¹⁾

Atypical MR imaging patterns have been described, in addition to the typical T1-hypointense and T2-hyperintense signal change. These include T1-isointense or hyperintense vertebral bodies and lack of endplate erosions, and T2-isointense or hypointense vertebral bodies. Atypical patterns of involvement include solitary vertebral body or discal involvement, single vertebral body and disc, or two adjacent vertebral bodies without intervening disc involvement. Age-related changes in the bone marrow can mask marrow oedema-related T1-hypointensity, necessitating the use of fat-suppression sequences, particularly on post-contrast T1-weighted MR images.⁽³⁾ During healing, there is a decrease in soft tissue inflammation, shown as a corresponding decrease in contrast enhancement, and an increase in fatty marrow replacement (increase in T1 signal intensity). These signal changes are not deemed as reliable indicators of healing.⁽³⁾

MR imaging is superior in the demonstration of paravertebral soft tissue masses (Fig. 8), most often being T1-hypointense, T2-heterogeneously hyperintense, and of epidural masses, which are slightly T1-hypointense and T2-hyperintense. Compression or displacement of the spinal cord should be looked for in the presence of epidural masses, which may show craniocaudal migration (Fig. 9). MR imaging findings with good to excellent sensitivity for infective spondylitis include the presence of paravertebral or epidural inflammatory tissue, intradiscal contrast enhancement, T2-signal hyperintensity or fluid-equivalent intensity, and erosion or destruction of the vertebral endplates on T1-weighted images. MR findings with low sensitivity include finding of a T1-hypointense disc, decrease in intervertebral disc height, and effacement of the intranuclear cleft.⁽⁵⁾

Three-phase bone scintigraphy using Technetium-99m methylene diphosphonate (Tc-99m MDP) is the most commonly-utilised radionuclide imaging technique, and is able to display local hyperaemia, increased blood pool activity, and increased uptake in the endplates. While sensitivity is fairly high (90%), specificity is low (72%), with degenerative disc disease being a frequent cause of false-positives. Gallium (Ga⁶⁷) scintigrams have a similar sensitivity and slightly better specificity (90%) than Tc-99m MDP bone scintigrams, showing increased radioactivity in the endplates and disc spaces.⁽⁹⁾

Fluorine-18-fluorodeoxyglucose positron emission tomography (FDG-PET) has been shown to be able to accurately detect acute and chronic osteomyelitis of the appendicular and axial skeleton. It is also able to

differentiate osteomyelitis from adjacent soft tissue infections,⁽¹⁰⁾ and between degenerative and infective endplate changes.⁽¹¹⁾ Its main drawback is the inability to differentiate infection from malignant lesions. Nonetheless, it is useful as a screening tool when a negative study will exclude the presence of infection and to show disease regression with therapy. It is also not hampered by the presence of metallic implants.

Tuberculous infection of the spine accounts for more than 50% of musculoskeletal TB. In tuberculous spondylitis, while the radiographical, CT, MR imaging and nuclear medicine imaging features are fairly similar to that of pyogenic spondylitis, attention should be paid to additional distinguishing findings. A primary focus elsewhere is usually present and should be searched for, with the most common sites being the lungs and genitourinary system. Pathological calcification is more commonly seen with tuberculous spondylitis on radiographs and CT. Discal involvement may not be present, resulting in preservation of disc height. Subligamentous spread is a particular feature of TB and is frequent, occurring in a craniocaudal manner and leads to skip vertebral involvement (4%) or non-contiguous multilevel involvement. Anterior vertebral scalloping with relative disc space preservation is a sign of subligamentous spread on lateral radiographs and CT.^(4,12)

Tuberculous infection may not be confined to the vertebral body only, unlike in pyogenic spondylitis, with the posterior elements showing signs of involvement (2%–10%). Isolated infection of the posterior arch is found in less than 2%.^(1,4,12) Paravertebral (75%) and epidural (61%) masses are more common (up to 75% of patients) than in pyogenic spondylitis, showing avid rim enhancement with enhanced T1-weighted sequences, and T2-weighted and STIR signal hyperintensity.^(1,12) The two most reliable MR imaging findings that are suggestive of tuberculous spondylitis are thin and smooth abscess wall enhancement and well-defined paravertebral abnormal signal intensity.⁽¹³⁾ Because of its slower disease progression, sclerosis and bony destruction is more common, with gibbus deformity (marked forward kyphosis of the spine), secondary to infective compression fracture, being quite frequently seen.⁽¹²⁾

The most important differential diagnosis is a neoplastic process, with imaging features that include preservation of disc space and effacement of paravertebral fat planes. Posterior element involvement and skip vertebral involvement can be found with neoplastic conditions and are not considered to be reliable discriminatory features.⁽¹⁾ Other differentials include

degenerative disc disease, pseudoarthrosis in ankylosing spondylitis, haemodialysis amyloid spondyloarthropathy and neuropathic spondyloarthropathy. In children, primary chronic recurrent multifocal osteomyelitis, a self-limiting condition, may show partial collapse of the vertebral body, marrow oedema, disc space narrowing, contrast enhancement of the vertebral body and skip vertebral involvement, but with no soft tissue involvement or abscess formation and a hypointense disc.⁽¹⁾

Paraplegia or tetraplegia is seen in 1% of patients with infective spondylitis.⁽⁴⁾ Less severe complications include gibbus deformity of the spine in tuberculous spondylitis, bony ankylosis, and neurological deficits from spinal cord involvement. In summary, infective spondylitis, whether pyogenic or tuberculous, is uncommon but should be actively excluded in patients with non-traumatic back pain. Blood tests, such as TWC, ESR and CRP, may be non-specific and at most, help suggest the presence of infection. Imaging, particularly MR imaging, remains essential for an accurate diagnosis, and is useful in follow-up for monitoring disease progression.

ABSTRACT

A 60-year-old Indian man presented with lower thoracic pain and bilateral lower limb weakness. Radiographs showed compression fractures of T8 and T9 and destruction of the T7 and T10 endplates. Magnetic resonance imaging confirmed the vertebral changes and showed subligamentous spread, paravertebral masses, and epidural involvement leading to cord compression. Computed tomography-guided biopsy showed granulomatous caseous necrosis and acid-fast bacilli, confirming the diagnosis of tuberculous spondylitis. The imaging features of infective spondylitis, with emphasis on tuberculous spondylitis, are discussed.

Keywords: infective spondylitis, pyogenic spondylitis, tuberculosis, tuberculous spondylitis, vertebral infection

Singapore Med J 2008;49(7):581-591

REFERENCES

1. James SLJ, Davies AM. Imaging of infectious spinal disorders in children and adults. *Eur J Radiol* 2006; 58:27-40.
2. Howard SA, Seldomridge JA. Spinal infections. Diagnostic tests and imaging studies. *Clin Orthop* 2006; 444:27-33.
3. Varma R, Lander P, Assaf A. Imaging of pyogenic infectious spondylodiskitis. *Radiol Clin North Am* 2001; 39:203-13.
4. Jetvic V. Vertebral infection. *Eur Radiol* 2004; 14:E43-E52.

5. Ledermann HP, Schweitzer ME, Morrison WB, Carrino JA. MR Imaging findings in spinal infections: rules or myths? *Radiology* 2003; 228:506-14.
6. Munk PL, Lee MJ, Poon PY, et al. Candida osteomyelitis and disc space infection of the lumbar spine. *Skeletal Radiol* 1997; 26:42-6.
7. Chhem RK, Wang SC, Jaovisidha S, et al. Imaging of fungal, viral and parasitic musculoskeletal and spinal diseases. *Radiol Clin North Am* 2001; 39:357-78.
8. Forrester DM. Infectious spondylitis. *Semin Ultrasound CT MRI* 2004; 25:461-73.
9. Turpin S, Lambert R. Role of scintigraphy in musculoskeletal and spinal infections. *Radiol Clin North Am* 2001; 39:169-89.
10. Kalicke T, Schmitz A, Risse JH, et al. Fluorine-18 fluorodeoxyglucose PET in infectious bone diseases: results of histologically confirmed cases. *Eur J Nucl Med* 2000; 27:524-8.
11. Stumpe KDM, Zanetti M, Weishaupt D, et al. FDG positron emission tomography for differentiation of degenerative and infectious endplate abnormalities in the lumbar spine detected on MR imaging. *Am J Roentgenol* 2002; 179:1151-7.
12. Gouliamos AD, Kehagias DT, Lahanis S, et al. MR imaging of tuberculous vertebral osteomyelitis: pictorial review. *Eur Radiol* 2001; 11:575-9.
13. Jung NY, Jee WH, Ha KY, et al. Discrimination of tuberculous spondylitis from pyogenic spondylitis on MRI. *Am J Roentgenol* 2004; 182:1405-10.

SINGAPORE MEDICAL COUNCIL CATEGORY 3B CME PROGRAMME
Multiple Choice Questions (Code SMJ 200807B)

	True	False
Question 1. Concerning infective spondylitis:		
(a) It accounts for at least 10% of cases of osteomyelitis.	<input type="checkbox"/>	<input type="checkbox"/>
(b) It classically involves two adjacent vertebrae and the intervening intervertebral disc.	<input type="checkbox"/>	<input type="checkbox"/>
(c) It is more common in children, with a bimodal age distribution.	<input type="checkbox"/>	<input type="checkbox"/>
(d) It more commonly affects the cervical spine, compared to the thoracic spine.	<input type="checkbox"/>	<input type="checkbox"/>
Question 2. In infective spondylitis:		
(a) Iatrogenic causes accounts for a considerable proportion of cases.	<input type="checkbox"/>	<input type="checkbox"/>
(b) <i>Streptococcus</i> spp. is the most common causative organism.	<input type="checkbox"/>	<input type="checkbox"/>
(c) <i>Staphylococcus aureus</i> is the most common organism in intravenous drug users.	<input type="checkbox"/>	<input type="checkbox"/>
(d) ESR and CRP levels have similar sensitivity as markers of infection.	<input type="checkbox"/>	<input type="checkbox"/>
Question 3. Regarding the imaging of infective spondylitis:		
(a) Radiographical changes correspond accurately to disease progression.	<input type="checkbox"/>	<input type="checkbox"/>
(b) Anterior vertebral body subchondral radiolucency is related to the venous supply to the vertebra.	<input type="checkbox"/>	<input type="checkbox"/>
(c) CT is more sensitive than radiographs for detection of paraspinal involvement.	<input type="checkbox"/>	<input type="checkbox"/>
(d) An accepted role for CT is in imaging-guided intervention and biopsy.	<input type="checkbox"/>	<input type="checkbox"/>
Question 4. Concerning MR imaging in spinal osteomyelitis:		
(a) It is generally recommended that the entire spine should be scanned.	<input type="checkbox"/>	<input type="checkbox"/>
(b) Intravenous contrast agent administration is not helpful in distinguishing infection from degenerative changes.	<input type="checkbox"/>	<input type="checkbox"/>
(c) Typical signal changes include hyperintense areas on T1-weighted, T2-weighted and STIR sequences.	<input type="checkbox"/>	<input type="checkbox"/>
(d) Infection spread into the spinal canal is just as readily detected on MR imaging as with CT.	<input type="checkbox"/>	<input type="checkbox"/>
Question 5. In tuberculous spondylitis:		
(a) Urological assessment may be necessary.	<input type="checkbox"/>	<input type="checkbox"/>
(b) Sub-ligamentous spread is a known characteristic finding and frequently occurs posteriorly.	<input type="checkbox"/>	<input type="checkbox"/>
(c) Involvement of the posterior elements of the vertebra is as common with tuberculous spondylitis as with <i>Staphylococcus aureus</i> spondylitis.	<input type="checkbox"/>	<input type="checkbox"/>
(d) Gibbus deformity and paravertebral calcification are late signs of tuberculous spondylitis.	<input type="checkbox"/>	<input type="checkbox"/>

Doctor's particulars:

Name in full: _____

MCR number: _____ Specialty: _____

Email address: _____

SUBMISSION INSTRUCTIONS:(1) Log on at the SMJ website: <http://www.sma.org.sg/cme/smj> and select the appropriate set of questions. (2) Select your answers and provide your name, email address and MCR number. Click on "Submit answers" to submit.**RESULTS:**(1) Answers will be published in the SMJ September 2008 issue. (2) The MCR numbers of successful candidates will be posted online at www.sma.org.sg/cme/smj by 15 September 2008. (3) All online submissions will receive an automatic email acknowledgment. (4) Passing mark is 60%. No mark will be deducted for incorrect answers. (5) The SMJ editorial office will submit the list of successful candidates to the Singapore Medical Council.**Deadline for submission: (July 2008 SMJ 3B CME programme): 12 noon, 25 August 2008.**